

## Fluorescence imaging and spectroscopy of motile sperm cells and CHO cells in an optical trap ("laser tweezers")

Karsten König<sup>1,2</sup>, Yagang Liu<sup>2,3</sup>, Tatjana Krasieva<sup>2</sup>, Pasquale Patrizio<sup>4</sup>,  
Yona Tadir<sup>1</sup>, Greg J. Sonek<sup>3</sup>, Michael W. Berns<sup>2</sup>, Bruce J. Tromberg<sup>2</sup>

<sup>1</sup>Institute for Molecular Biotechnology, D-07708 Jena, Germany

<sup>2</sup>Beckman Laser Institute and Medical Clinic, University of California, Irvine, CA 92715

<sup>3</sup>Department of Electrical and Computer Engineering, University of California, Irvine, CA 92715

<sup>4</sup>Department of Obstetrics and Gynecology, University of California, Irvine, CA 92715

### 1. ABSTRACT

We describe fluorescence spectroscopy and imaging studies of optically trapped single Chinese hamster ovary (CHO) and motile human sperm cells. The NIR trapping beam was provided by a tunable, multimode continuous wave Ti:Sapphire laser. The beam was introduced into an inverted confocal laser scanning microscope. Fluorescence of cells in the single-beam gradient force optical trap was excited with a 488 nm microbeam (laser scanning microscopy) or with 365 nm radiation from a high-pressure mercury lamp. Modifications to NADH-attributed autofluorescence and Rhodamine- and Propidium Iodide-attributed xenofluorescence indicate a significant cell-damaging effect of 760 nm trapping beams. 760 nm effects produce a biological response comparable to UVA-induced oxidative stress and appear to be a consequence of two-photon absorption.

**Keywords:** optical trapping, fluorescence, microbeam, NADH, laser scanning microscopy, two-photon excited fluorescence, photostress, UVA, NIR, oxidative stress

### 2. INTRODUCTION

Optical cell trapping ("optical tweezers") is a novel technique based on force generation during intracellular refraction of microbeams (ray-optics model)<sup>1,2</sup>. These trapping forces  $F$  can be determined by  $F=QP/c$ , where  $c$  is the light speed in medium, and  $Q$  an efficiency parameter which depends on optical properties of the trapped object and on laser beam quality. In order to confine a highly motile cell, such as a sperm cell, the trapping forces should be higher than the intrinsic, ATP-driven motility forces. With typical motility forces of human sperm cells of 40 pN and  $Q$ -values of about 0.1 for single-beam gradient force optical traps (objective with numerical aperture (NA) of 1.3), laser powers at the sample of 50-200 mW are required to confine motile spermatozoa<sup>3</sup>. When "immobilized" in the trap, cell micromanipulation, optical force measurement, and intracellular fluorescence detection is possible.

This paper reports on fluorescence spectroscopy and fluorescence imaging of vital single cells in an optical trap. Fluorescence detection was used to evaluate cellular response on UVA and NIR photostress. In particular, we investigated the pathophysiological effects of near-infrared (NIR) trapping beams. Microbeams can create an enormous intracellular photon flux. A highly focused continuous wave (CW) 100 mW trapping beam at 760 nm (NA= 1.3) leads to intensities of about 40 MW/cm<sup>2</sup> and in the course of a 1 min experiment, radiant exposures of 2 GJ/cm<sup>2</sup> can be achieved. Both, externally applied fluorescent probes (xenofluorescence) and intrinsic fluorescent coenzymes (autofluorescence), such as the reduced pyridine coenzymes  $\beta$ -nicotinamide adenine dinucleotide (NADH) and  $\beta$ -nicotinamide adenine dinucleotide phosphate (NADPH), were employed as sensitive bioindicators of metabolic function<sup>4-6</sup> during NIR and UVA irradiation..

### 3. MATERIALS AND METHODS

*Chemicals.* Cells were labeled with the mitochondrial activity marker Rhodamine 123 (Rh, 10  $\mu\text{M}$ ), the single-stranded DNA-damage indicator Acridine Orange (AO, 3  $\mu\text{M}$ ), and with the LIVE/DEAD FertiLight™ Sperm Viability Kit (Molecular Probes). The viability kit contains the membrane-permeable nucleic acid, live-cell stain SYBR™14 (100 nM) with an emission maximum at 515 nm and the dead-cell stain Propidium Iodide (PI, 12  $\mu\text{M}$ ) with an emission maximum at 636 nm. The fluorophore 6-dodecanoyl-2-dimethylaminonaphthalene (Laurdan, 2  $\mu\text{M}$ , Molecular Probes), which binds to phospholipids of cellular membranes and which exhibits a temperature-sensitive fluorescence maximum, was used for nondestructive intracellular temperature measurements. To quantify the photoinduced temperature increase, the "General Polarization (GP)" was used with  $\text{GP} = (I_{440\text{nm}} - I_{490\text{nm}}) / (I_{440\text{nm}} + I_{490\text{nm}})$ , where  $I_{440\text{nm}}$  and  $I_{490\text{nm}}$  are the Laurdan fluorescence intensities at the maximum emission in gel and liquid-crystalline phase when embedded in the phospholipid bilayer of dipalmitoyl-phosphatidyl choline (DPPC) liposomes<sup>7,8</sup>.

*Cell and cell culture.* Chinese hamster ovary cells (CHO, ATCC no. 61) were maintained in GIBCO's minimum essential medium (MEM, 10% fetal bovine serum). Cells were subcultured in T-25 tissue culture flasks twice a week using 0.25% trypsin for desiccation. For experimentation, trypsinized cells were diluted in PBS, pH= 7.4, and injected into a modified Rose culture chamber. Semen specimens were obtained from three donors with normal semen parameters according to the World Health Organization guidelines. Semen was diluted in HEPES buffered isotonic saline solution containing 1% human serum albumin. Spermatozoa were injected into microchambers. Experiments were performed within three hours following ejaculation at a room temperature of 29°C.

*Experimental set-up.* The NIR radiation of an Ar<sup>+</sup>-ion laser-pumped tunable Ti:Sapphire ring laser (Coherent, models innova 100, and 899-01) was introduced into a modified inverted confocal laser scanning microscope (CLSM, Axiovert 135M, Zeiss). The parallel beam was expanded to fill the back aperture of a 100x Zeiss Neofluar brightfield objective (NA=1.3). Laser scan images were obtained with 488 nm microbeams of an Ar<sup>+</sup>-ion laser with a power at the sample of 2.2  $\mu\text{W}$  and a scanning time of 1s per image. The microscope (Fig. 1) allows trapping of single cells and simultaneous laser scanning for transmission brightfield- and xenofluorescence imaging of chromophores with absorption bands in the blue/green spectral region. For autofluorescence imaging, the UV excited fluorescence was detected with a slow-scan, cooled CCD camera (TE576/SET135, Princeton Instruments) or cooled-color CCD camera (ZVS-47DEC, Zeiss). A 50 W high-pressure mercury arc lamp equipped with an IR blocking filter and a 365 nm bandpass filter served as the autofluorescence excitation source. The UVA power was determined to be 1.0 mW, the diameter of the circular irradiation area to be 0.190 mm. However, the power measured after the objective in air is different from the real power at the sample due to different water and glass refractive indices. As a result, a correction factor of 1.5 was applied for both, UV and NIR radiation<sup>3</sup>. Therefore, the UVA intensity was estimated to be 5.3  $\text{W}/\text{cm}^2$  at the sample.

The spot size of the focused NIR microbeam in the microscope was found to be  $<1 \mu\text{m}$  as measured with the CCD camera using the reflex on the cover slip. More accurate, previously measured spot sizes using the knife-edge technique<sup>9</sup>, revealed a size of  $0.78 \pm 0.06 \mu\text{m}$  for this objective for 1064 nm beams. We therefore assumed diffraction-limited spots in our work could be approximated by  $d = \lambda/1.3$ .

Intracellular spectra were obtained using another experimental set-up with a 1064 nm trapping beam and a polychromator combined with a cooled optical multichannel analyzer for spectra recording. Fluorescence was excited with 365 nm mercury lamp radiation ( $1 \text{ W}/\text{cm}^2$ ). Each spectrum was acquired in 5 s and corrected using an NBS-calibrated light source. This set-up is described in detail in refs.(8) and (10).

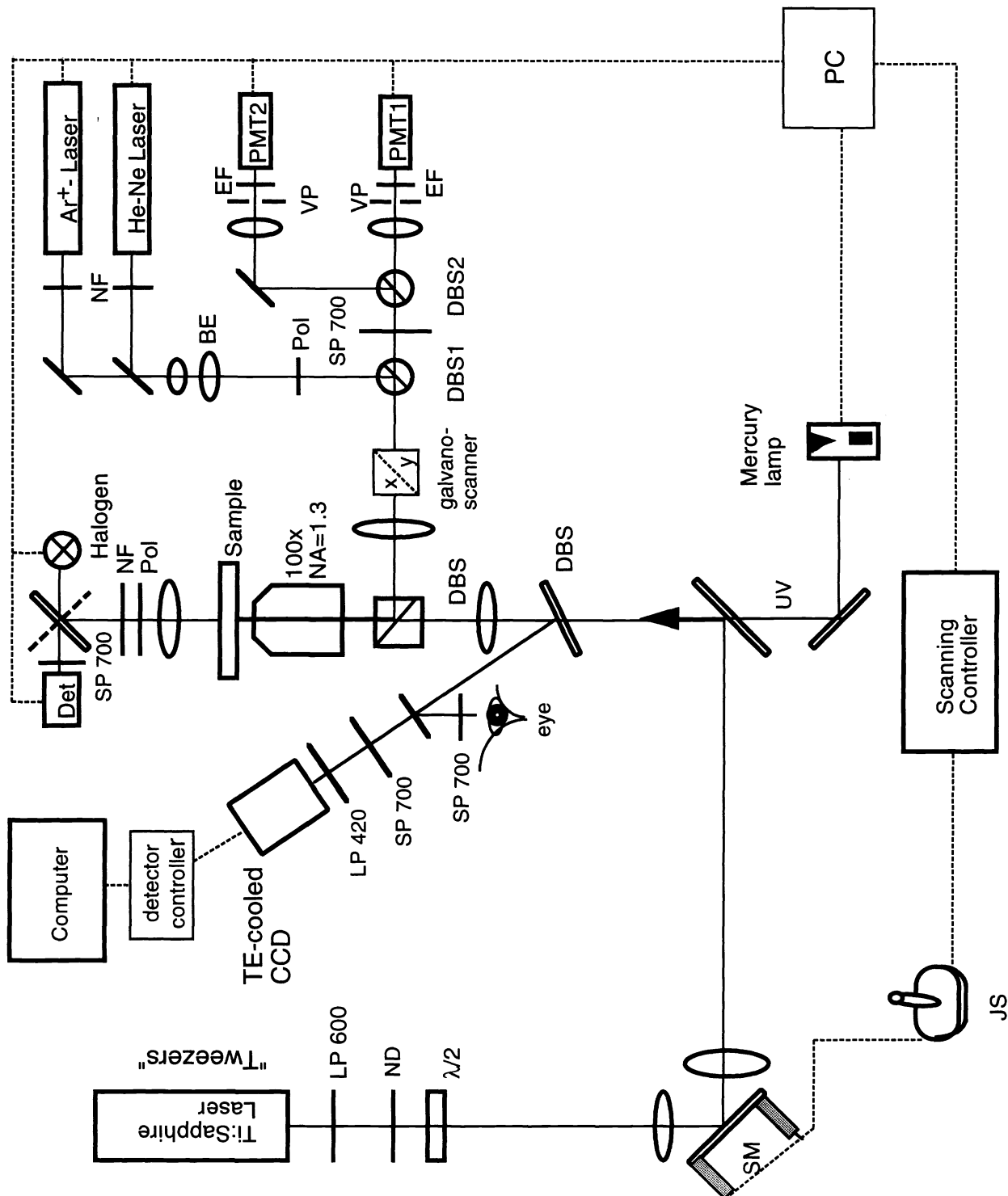


Fig. 1 Scheme of the modified laser scan microscope for sensitive fluorescence imaging of single cells in a NIR gradient force optical trap.

ND: neutral density filter, SM: scan mirror, JS: joystick, SP: short pass filter, Pol: polarizer, DBS: dichroic beamsplitter, BE: beam expander, EF: emission filter, VP: pinhole, Det: detector, PMT: photomultiplier, PC: personal computer

## **4. RESULTS**

### **4.1. Autofluorescence imaging of optically-trapped CHO cells**

CHO cells (mean diameter: 11  $\mu\text{m}$ ) were confined in a 760 nm trap (100 mW) and briefly (1 s) exposed to 365 nm radiation to excite cellular autofluorescence at time intervals of 5 min. Fluorescence images showed strong signals within the cytoplasm. Interestingly, the autofluorescence image changed during trapping. The third image, obtained after 10 min trapping, indicates the formation of a spatially-limited intense autofluorescence spot (Fig. 2). With time, the intracellular area of enhanced fluorescence and the fluorescence intensity increased. Integrated autofluorescence (mean cellular fluorescence intensity) increased two-fold after 20 min of trapping, and the fluorescence intensity within the fluorescent spot (corresponding to an area of about 1  $\mu\text{m}^2$ ) increased up to four-fold compared with initial levels. In contrast, 800 nm trapping beams did not induce such significant autofluorescence changes.

UVA exposure (365 nm) to trapped cells resulted in immediate autofluorescence changes. For radiant exposures up to 50  $\text{J}/\text{cm}^2$ , cellular autofluorescence intensity decreased. Further exposure led to a four-fold fluorescence increase (Fig. 3) compared with the initial fluorescence intensity.

### **4.2. Fluorescence spectroscopy of optically-trapped CHO cells**

Autofluorescence spectra of a CHO cell in an optical trap were recorded in order to study the influence of the 1064 nm trapping beam and UVA exposure on cellular redox state. The autofluorescence spectrum of unexposed cells exhibited a broad band (bandwidth:  $\approx 60$  nm) with a peak at 455 nm. This peak reflects the blend of free and bound NAD(P)H in the cell. Free NAD(P)H emits in aqueous solution around 460 nm, whereas protein-bound NAD(P)H fluoresces around 440 nm<sup>10</sup>. No significant spectral changes of cellular autofluorescence were obtained during trapping with 1064 nm microbeams (230 mW) even for radiant exposures up to 120  $\text{GJ}/\text{cm}^2$  (measurements in periods of 5 min). However, UVA exposure resulted in modifications of fluorescence intensity and in a red-shift of the fluorescence maximum of 7 nm (Fig. 4).

In order to achieve information on intracellular temperature increase during photostress, cells were labeled with the thermosensitive fluorophore Laurdan. Fig. 5 shows the fluorescence maximum and the GP-value of Laurdan-doped liposomes (phospholipid bilayer) versus temperature indicating GP-changes of 0.39/K in the phase transition region, and 0.03/K for higher temperatures<sup>8</sup>. In contrast, GP-changes of 0.01/K in the temperature region of 20°C - 45°C occur in Laurdan-labeled CHO cells due to dye accumulation in various cellular phospholipids (Fig. 6, left). Previous measurements<sup>11</sup> on optically-trapped liposomes and CHO cells showed that the 1064 nm microbeam induces a mean cellular temperature increase of 2 K per 100 mW. This temperature increase occurred within seconds. For the determination of the intracellular temperature increase of UVA light alone (no NIR exposure), Laurdan labeled, glass-attached CHO cells were used. As demonstrated in Fig. 6 right, UVA exposure (1  $\text{W}/\text{cm}^2$ ) using a 100x objective with oil immersion led within 1 min to a temperature increase of 3 K. However, this temperature change is based on cellular absorption as well as on indirect heating due to strong absorption by the immersion oil. Using an objective with water immersion, temperature changes are less than 1 K. Therefore, UVA-induced autofluorescence changes are based on photochemical and not on thermal effects. A disadvantage of the thermosensor Laurdan is the photoinstability (photobleaching) during UV exposure.

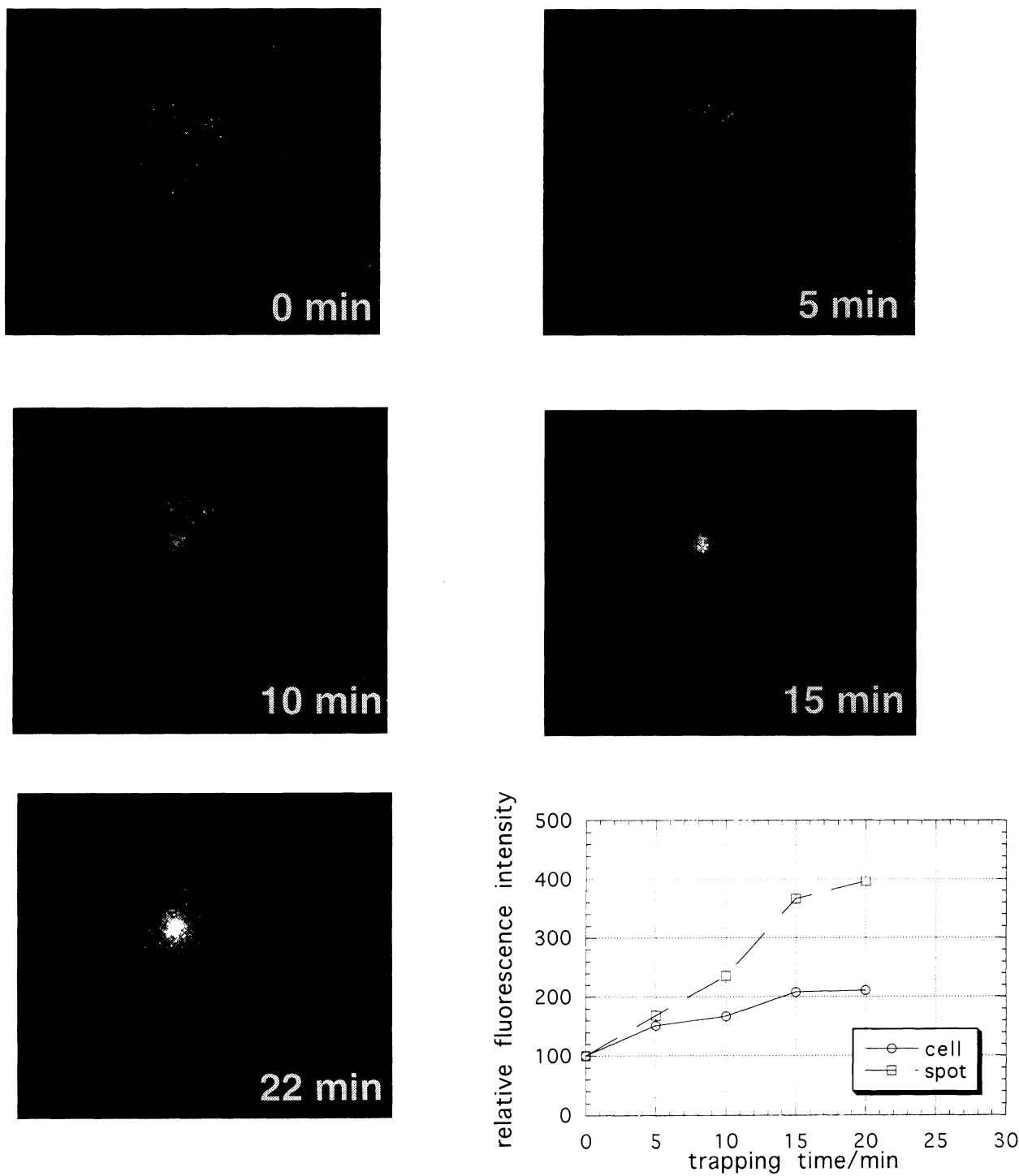


Fig. 2 Autofluorescence imaging of CHO cells in a 760 nm trap. The fluorescence pattern depends on trapping time. The diagram shows the mean fluorescence intensity of the entire cell and of a 1  $\mu$ m spot (region of highest fluorescence intensity)

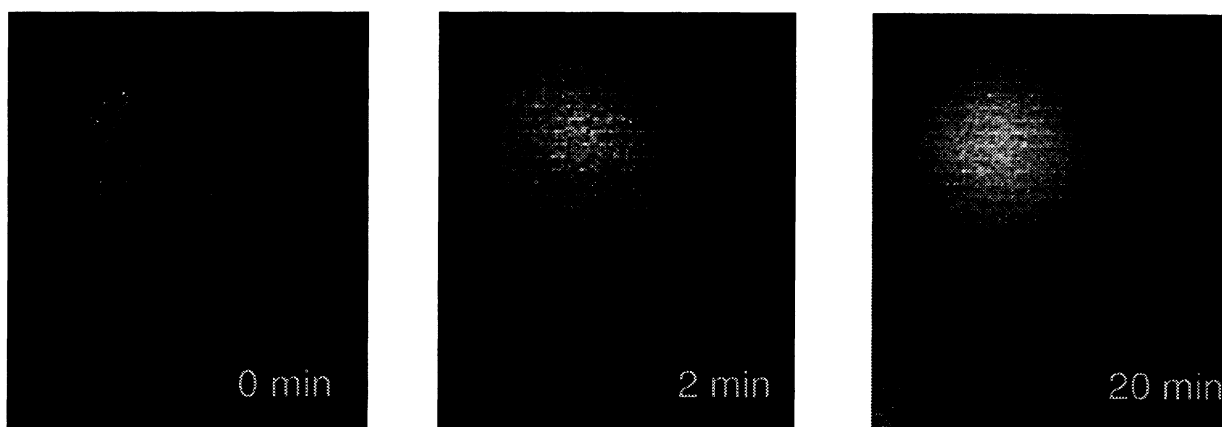


Fig. 3 Autofluorescence modifications of optically-trapped CHO cells during UVA stress.

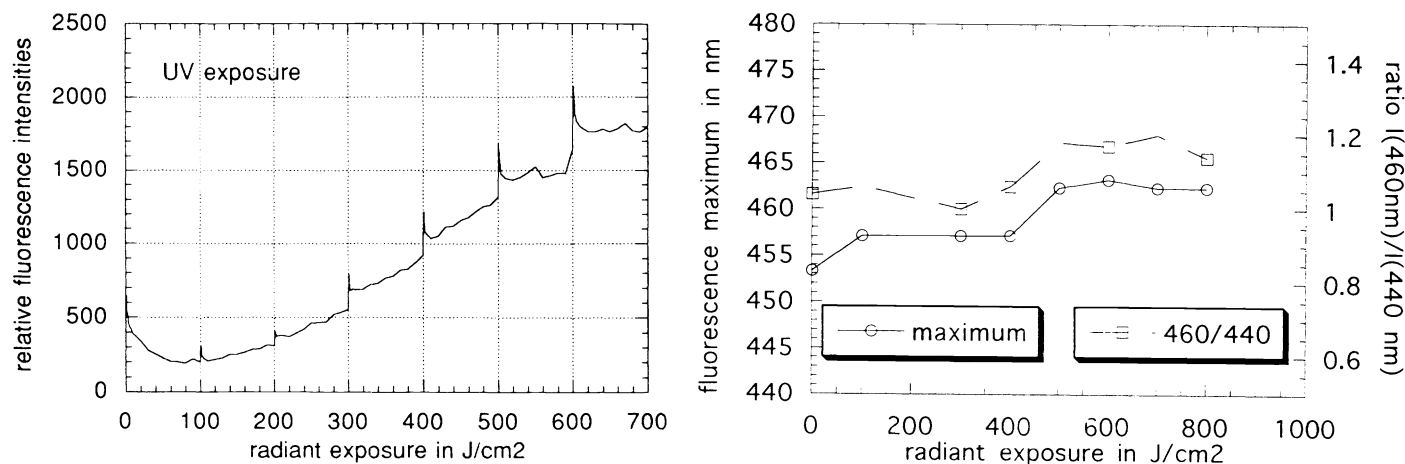


Fig. 4 Autofluorescence spectroscopy during UVA stress. Up to 1200 spectra (in series of 100) were recorded during 365 nm exposure to optically-trapped CHO cells. The left figure shows intensity modifications at 450 nm, the right figure exhibits shifts of the fluorescence maximum and shows the ratio of free to bound NAD(P)H versus UVA radiant exposure.

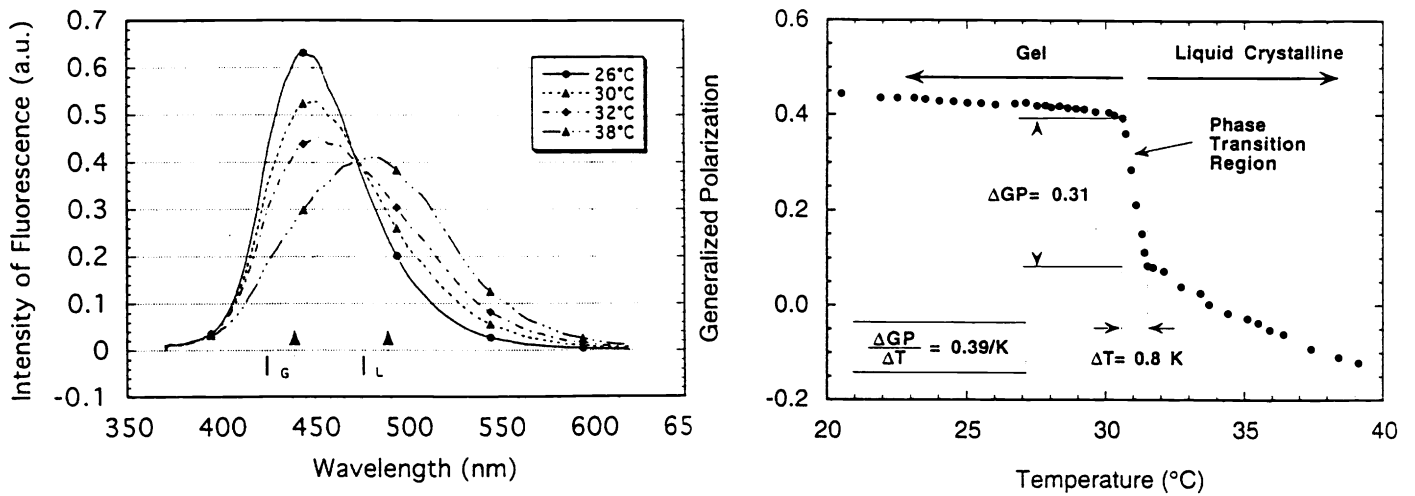


Fig. 5 Fluorescence spectra (left) and General Polarization (GP, right) of Laurdan-doped liposomes versus temperature.

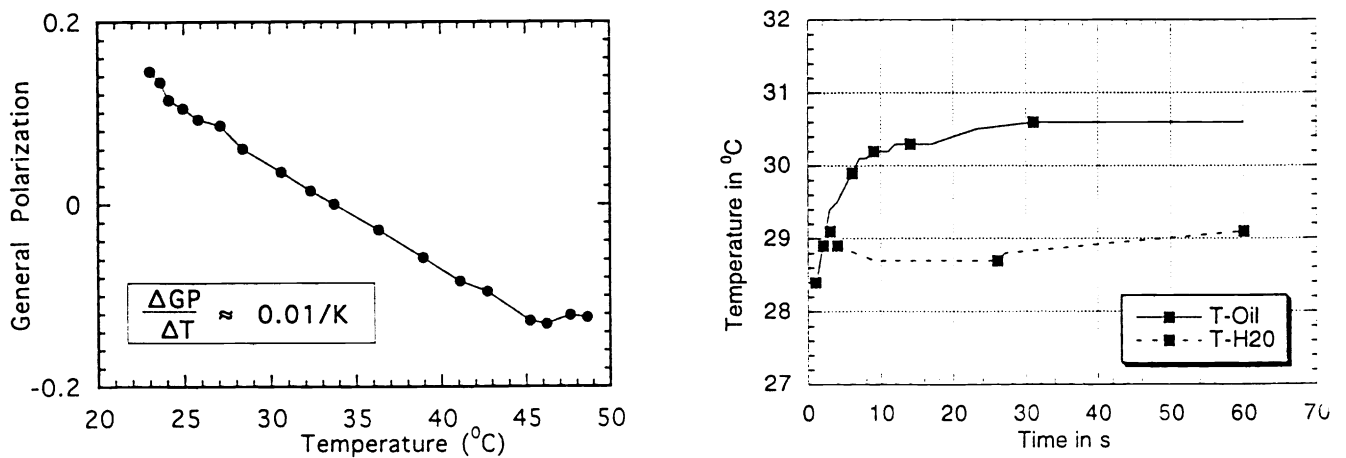


Fig. 6 General Polarization (GP) of Laurdan-labeled cells versus temperature (calibration curve, left) and temperature changes in Laurdan-labeled CHO cells during UVA-exposure (right).

### **4.3. Fluorescence imaging and spectroscopy of motile spermatozoa**

Motile human sperm cells were trapped with a 150 mW microbeam (800 nm) while 365 nm-excited autofluorescence was imaged with the slow-scan CCD camera. Motile spermatozoa autofluorescence was located in the mid-piece of the cell (Fig. 7). The sperm mid-piece is known to be the primary site for mitochondria which contain high amounts of fluorescent NAD(P)H. Interestingly, the fluorescence intensity increased and appeared to relocalize with UVA irradiation. The sperm head became the brightest fluorescent site. Autofluorescence spectra of single, optically trapped sperm cells before and after UVA exposure exhibited the increase, however, no significant changes in spectral characteristics occurred (Fig. 8). These autofluorescence modifications correlated with a loss of motility. A mean UVA radiant exposure of about  $570 \pm 160 \text{ J/cm}^2$  ( $n = 10$ ) was determined for the onset of paralysis.

Interestingly, non-UVA-exposed sperm cells in a 760 nm trap (105 mW) stopped movement after  $35 \pm 20 \text{ s}$  ( $n = 10$ ). The autofluorescence pattern of these paralyzed spermatozoa are similar to those of UVA-exposed cells. In contrast, 90% of spermatozoa ( $n = 10$ ) in an 800 nm trap of same power kept motility up to 10 min trapping time.

Cell labeling with the fluorescent biosensors AO, Rh, and SYBR/PI allowed laser scanning fluorescence microscopy of spermatozoa in an optical trap (Fig. 9). The 488 nm excited green/red emission of the Live/Dead fluorophores was recorded with two photomultipliers in two spectral ranges 510-525 nm and 630-700 nm, respectively. Red fluorescence, indicating cell death by intranuclear PI accumulation, began to appear in the lower head section and spread with time throughout the entire head. Onset of red fluorescence of sperm cells ( $n = 10$ ) in an 760 nm trap (105 mW) occurred after a mean time of  $65 \pm 21 \text{ s}$ , in an 800 nm trap (105 mW)  $>10 \text{ min}$ , and during UVA exposure after  $310 \pm 110 \text{ s}$  (800 nm trap).

Rh labeled cells showed reduced fluorescence intensity with exposure time, and AO-labeled cells exhibited green fluorescence. No intracellular red emission (single strand breakage) of AO-labeled cells was detected for NIR-radiant exposures up to  $30 \text{ GJ/cm}^2$ .

Interestingly, optically-trapped sperm cells exhibited luminescence in a submicron-sized region in the sperm head without any further light exposure (Fig. 10). No such emission was found in non-trapped cells. In the case of Life/Dead labeled cells, the emission spot changed color from green to red in correlation with loss of vitality. The emission was more intense in 760 nm traps than in 800 nm traps.

### **4.4. Laser output measurements**

We found evidence for the presence of subnanosecond pulses with repetition frequencies of multiples of 180 MHz in the output of our "CW" Ti:Sapphire ring laser using a 1 GHz avalanche photodiode (model 1651, Ne Focus) and 1 GHz oscilloscope (DSA 601, Tektronix). The most intense pulses with a pulse width less than 500 ps (resolution limited due to detection system) were found for 760 nm radiation in contrast to all other wavelengths in the tuning range of 700-900 nm (Fig. 11).

## **5. DISCUSSION**

We performed fluorescence imaging and spectroscopy of single cells in an optical trap and demonstrated that optical traps can be combined with sensitive fluorescence detection for studying single motile cells or cell organelles. Auto- and xenofluorescence detection of cells in an optical trap provided information on cellular temperature, mitochondrial activity, DNA damage, redox state, and viability during photostress. The use of NIR microbeams for single-beam gradient force trapping and the simultaneous application of microbeams as fluorescence excitation sources allowed laser scanning microscopy of optically-trapped samples.

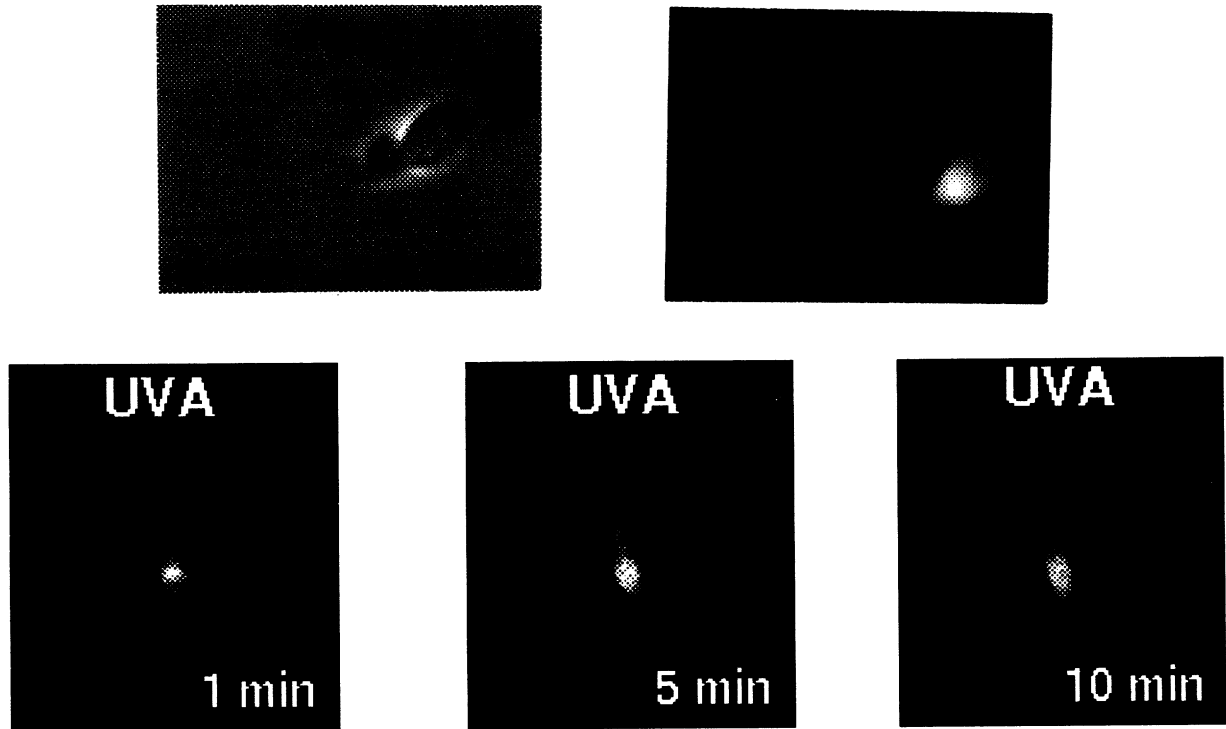


Fig. 7 Autofluorescence and transmission images of a single motile sperm confined to an 800 nm trap. UVA exposure results in fluorescence relocalization and increased fluorescence intensity.

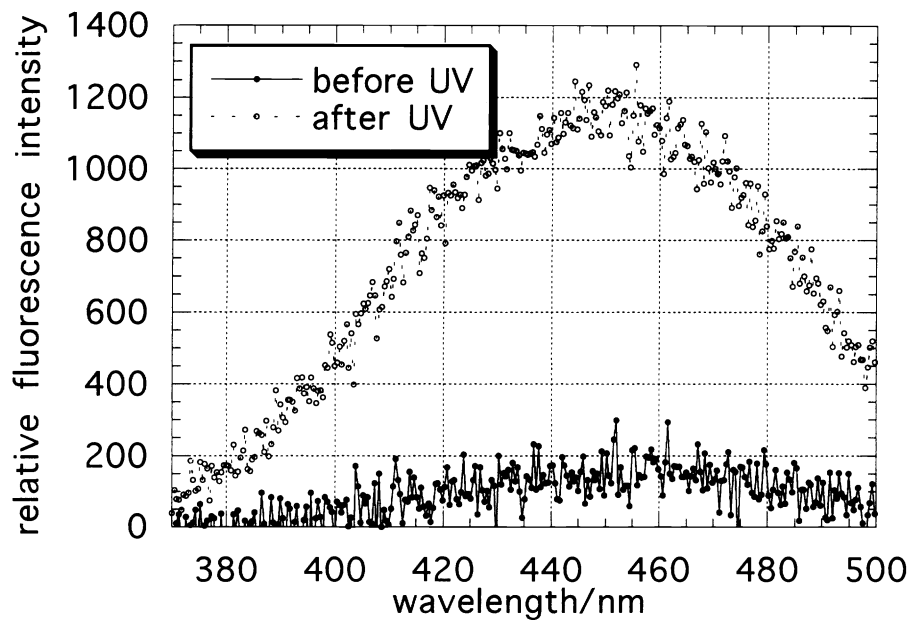


Fig. 8 Autofluorescence spectra of human sperm before and after UVA exposure.

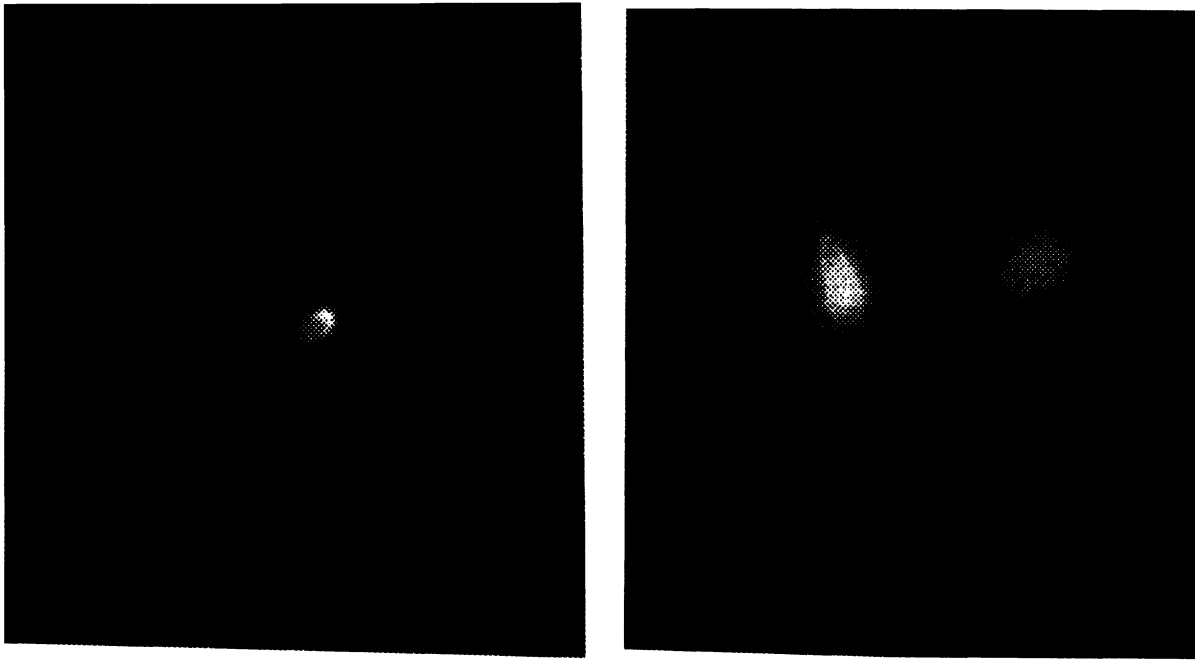


Fig. 9 Laser scanning fluorescence images of PI labeled sperm cells in the trap.

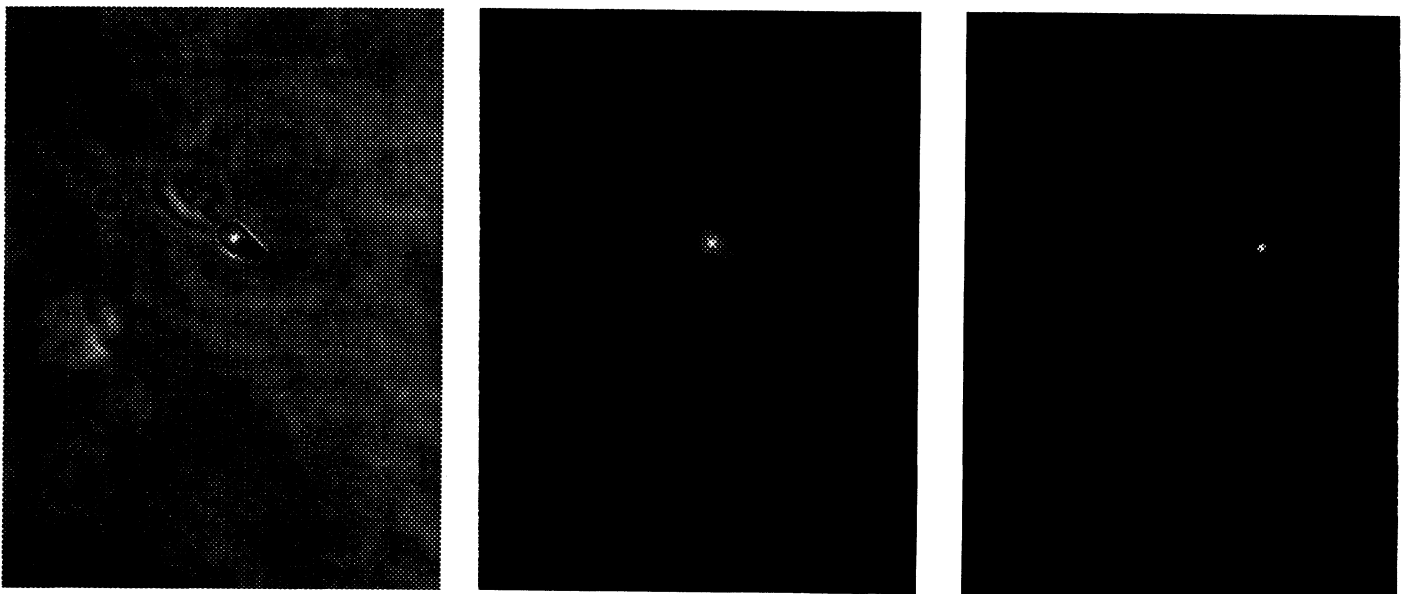


Fig. 10 NIR trapping beams induce two-photon excited fluorescence in trapped cells.  
left: brightfield image of Life/Dead labeled sperm cell in 760 nm trap  
middle: UVA-excited fluorescence (one-photon excitation)  
right: NIR-excited fluorescence (two-photon excitation)

Interestingly, NIR-induced emission in the visible spectral region was observed in trapped cells which can be explained by a non-linear, two-photon absorption process. Indeed, we found in recent experiments on NIR-induced emission of Rhodamine solution using a CW Ti:Sapphire laser, a squared dependence of fluorescence intensity on laser power<sup>12</sup>. Two-photon excited fluorescence requires photon flux densities of about  $10^{25}$  photons  $\text{cm}^{-2}\text{s}^{-1}$  (13, 14). A highly-focused CW microbeam at 760 nm provides about two orders higher photon flux density. However, the observed phenomena of 760 nm microbeams compared with 800 nm microbeams are based on different output characteristics of our "CW" laser. At a certain position of the birefringent filter which corresponds to 760 nm tuning, the laser provides intense subnanosecond pulses with pulse widths less than 500 ps. Pulse amplitude and repetition frequency can vary with time. Because multiphoton-absorption efficiency is strongly dependent on pulse amplitude, the observed 760 nm effects in sperm cells can be explained by a two-photon absorption process. Consequently, the effects of longitudinal mode beating should be considered in most "CW" laser microbeams, unless these sources are equipped with an etalon providing single-mode operation.

As demonstrated, one-photon UVA excitation and two-photon NIR excitation results in severe cell damage as probed by fluorescence imaging and fluorescence spectroscopy. In particular, NAD(P)H attributed autofluorescence was found to be a sensitive tool for monitoring cellular metabolism.

It is well known that UVA exposure results in oxidative stress<sup>15</sup>. Efficient absorbers in this spectral region are endogenous porphyrins (including metallo-porphyrins), pyridine and flavin molecules. These biomolecules may induce cell damage via charge transfer (type-I photooxidation) or energy transfer (type-II photooxidation). NIR microbeams may also induce oxidative stress via multiphoton-processes. Wavelengths shorter than 800 nm, therefore, do not appear to be appropriate for optical cell trapping.

## **6. ACKNOWLEDGMENTS**

This work was supported by the Office of Naval Research (N00014-91-0134), the Department of Energy (DE-FG-3-91-ER61227), the National Institutes of Health (5P41RR01192-15) and *Deutsche Forschungsgemeinschaft*. The authors are grateful to Norman Goldblatt for his helpful discussions.

## **7. REFERENCES**

1. A. Ashkin, "Acceleration and Trapping of Particles by Radiation Pressure", *Phys. Rev. Lett.* 24, 156-159, 1970.
2. A. Ashkin, J.M. Dziedzic, J.E. Bjorkholm, S. Chu, "Observation of a single-beam gradient force optical trap for dielectric particles", *Opt. Lett.* 11, 288-190, 1986.
3. K. König, L. Svaasand, Y. Liu, G.J. Sonek, P. Patrizio, J. Tadir, M.W. Berns, B.J. Tromberg, "Determination of intrinsic forces of human spermatozoa using an optical dynamometer", in preparation.
4. B. Chance and B. Thorell, "Localization and kinetics of reduced pyridine nucleotides in living cells by microfluorimetry.", *J. Biol. Chem.* 234, 3044-3050, 1959.
5. H. Schneckenburger, P. Gessler, I. Pavenstädt-Grupp, "Measurement of mitochondrial deficiencies in living cells by microspectrofluorometry", *J. Histochem. Cytochem.* 40(10), 1573-1578, 1992.
6. H. Schneckenburger, K. König, "Fluorescence decay kinetics and imaging of NAD(P)H and flavins as metabolic indicators", *Opt. Eng.* 31(7), 1447-1451, 1992.
7. T. Parasassi, G. De Stasio, A. d'Ubaldo, E. Gratton, "Phase fluctuation in phospholipid membranes revealed by Laurdan fluorescence", *Biophys. J.* 57(6), 1990, 1179-1186.
8. Y. Liu, D. Cheng, G.J. Sonek, B. J. Tromberg, M.W. Berns, "A microspectroscopic technique for the determination of localized heating effects in organic particles", *Appl. Phys. Lett.*, 65, 919, 1994.
9. W.H. Wright, G.J. Sonek, M.W. Berns, "Parametric study of the forces on microspheres held by optical tweezers", *Appl. Optics* 33, 1735-1748, 1994.

10. K. König, Y. Liu, G.J. Sonek, M.W. Berns, B.J. Tromberg, "Autofluorescence spectroscopy of optically-trapped (Laser Tweezers) cells during light-stress", SPIE-Proceedings, vol. 2329, in press.
11. Y. Liu, D.K. Cheng, G.J. Sonek, M.W. Berns, C.F. Chapman, B.J. Tromberg, "Evidence for Localized Cell Heating Induced by Infrared Optical Tweezers", Biophys. J., in press.
12. K. König, M.W. Berns, B.J. Tromberg, "Multi-Photon Absorption in Near Infrared Optical Traps", submitted.
13. J.P. Hermann, J. Ducuing, "Absolute Measurement of Two-Photon Cross Sections", Phys. Rev. A5, 2557-2568, 1972.
14. S.M. Kennedy, F.E. Lytle, "p-Bis(o-methylstyryl)benzene as a power squared sensor for two-photon absorption measurements between 537 and 694 nm", Anal. Chem. 58, 2643-2647, 1986.
15. R.M. Tyrrell, S.M. Keyse, "The interaction of UVA radiation with cultured cells", J. Photochem. Photobiol. B. 4, 349-361, 1990.

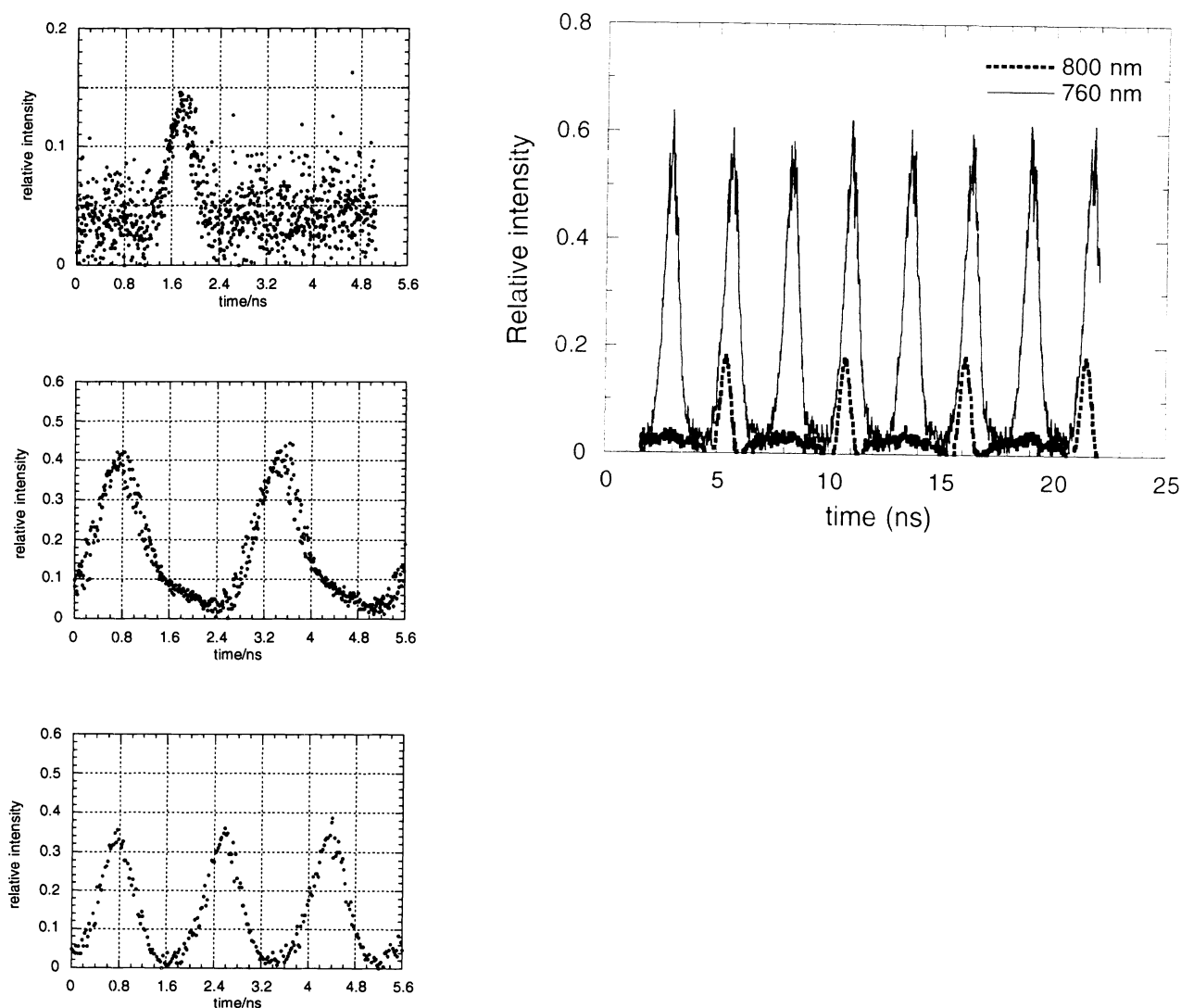


Fig. 11 Ti:Sapphire laser output. Presence of sub-nanosecond pulses at multiples of the base frequency (180 MHz) is shown. Pulse amplitude depends on wavelength.